N91-30234

FIESTA ROC: a New Finite Element Analysis Program for Solar Cell Simulation

Ralph O. Clark
Space Photovoltaic Research Center*, Electrical Engineering Department
Cleveland State University
Cleveland, Ohio

INTRODUCTION

FIESTA ROC (FInite Element Semiconductor Three-dimensional Analyzer by Ralph O. Clark) is a computational tool for investigating in detail the performance of arbitrary solar cell structures. As its name indicates, it uses the finite element technique to solve the fundamental semiconductor equations in the cell. It may be used for predicting the performance (thereby dictating the design parameters) of a proposed cell or for investigating the limiting factors in an established design.

THE FINITE ELEMENT METHOD

The fundamental semiconductor equations solved by FIESTA ROC are [1]

$$\nabla \cdot (\epsilon \mathcal{E}) = \rho \qquad \text{(Poisson's Equation)} \tag{1a}$$

$$\nabla \cdot \mathcal{F}_n = G - R \qquad \text{(Electron Continuity Equation)} \tag{1b}$$

$$\nabla \cdot \mathcal{F}_p = G - R \qquad \text{(Hole Continuity Equation)} \tag{1c}.$$

Here $\mathcal{E}$ is the electric field, ϵ the permittivity, ρ the volume charge density, $G - R$ the net carrier generation rate (generation minus recombination), and $\mathcal{F}_n$ and $\mathcal{F}_p$ the electron and hole flux densities. In turn, $\mathcal{E}$, $\mathcal{F}_n$, and $\mathcal{F}_p$ are related to the electrostatic potential ψ and the quasi-Fermi potentials ϕ_n, ϕ_p by

$$\mathcal{E} = -\nabla \psi \tag{2a}$$

$$\mathcal{F}_n = n_i \mu_n e^{(\psi - \phi_n)/V_T} \nabla \phi_n \tag{2b}$$

$$\mathcal{F}_p = -n_i \mu_p e^{(\phi_p - \psi)/V_T} \nabla \phi_p \tag{2c}.$$

As boundary conditions, we assume that the domain of simulation, Ω, has a boundary $\partial\Omega$ that can be partitioned into two segments: the Dirichlet boundary $\partial\Omega_D$, on which ψ, ϕ_n, and ϕ_p are prescribed, and the Neumann boundary $\partial\Omega_N$, on which the components of $\nabla\psi$, $\nabla\phi_n$, and $\nabla\phi_p$ normal to the surface all vanish. In particular, on the Dirichlet boundary, which corresponds to the contacts of a device, an infinite surface recombination velocity is assumed, pinning n and p to their levels at thermal equilibrium and ϕ_n and ϕ_p both to $\psi - \psi_0$. On the Neumann boundary, arbitrary surface recombination velocities are possible. Note that, for a one-dimensional model of a two-terminal device under these assumptions, we cannot model finite surface recombination velocities at the ends of the device because both ends represent contacts, i.e. Dirichlet boundaries.

Equations (1) can all be written in the generic form

$$\nabla \mathbf{f} - s = 0 \tag{3}.$$

To solve (3) by the finite element method, we first write it in its weak form, as follows. Let w be an arbitrary piecewise-continuous function on Ω, vanishing identically on $\partial\Omega_D$. Multiplying (3) by w, integrating over the entire volume, and integrating the first term by parts, we obtain

$$0 = \int_\Omega w(\nabla \cdot \mathbf{f} - s) = \int_{\partial\Omega} w\mathbf{f} \cdot \mathbf{n} - \int_\Omega (\nabla w \cdot \mathbf{f} + ws),$$

*funded by NASA Lewis Research Center, Cleveland, Ohio

where $\mathbf{n}$ is the unit outward normal to the surface. Note that since w vanishes on the Dirichlet boundary and $\mathbf{f} \cdot \mathbf{n}$ on the Neumann boundary, the surface integral vanishes, leaving us with the weak form of equation (3):

$$\int_\Omega (\nabla w \cdot \mathbf{f} + ws) = 0 \tag{4}.$$

We now discretize the problem by fixing N points, called nodes, between which w, ψ, ϕ_n, and ϕ_p all vary in a continuous way. In particular, we express $w\{\psi, \phi_n, \phi_p\}$ as a linear combination of continuous, piecewise smooth functions $W_i\{\Psi_i, \Phi_i^n, \Phi_i^p\}$, $i = 1, \ldots, N$, each of which assumes the value of 1 at node i and zero at all other nodes. Thus, $w = \sum_{i=1}^N w_i W_i$, $\psi = \sum_{i=1}^N \psi_i \Psi_i$, $\phi_n = \sum_{i=1}^N \phi_i^n \Phi_i^n$, $\phi_p = \sum_{i=1}^N \phi_i^p \Phi_i^p$, where the w_i are arbitrary coefficients (to keep w arbitrary) and ψ_i, ϕ_i^n, ϕ_i^p are just the values assumed by ψ, ϕ_n, and ϕ_p at node i. Now equation (4) becomes

$$\sum_{i=1}^N w_i \int_\Omega (\nabla W_i \cdot \mathbf{f} + W_i s) = 0 \tag{5}.$$

Since the N coefficients w_i are arbitrary, equation (5) really represents the system of N equations

$$\int_\Omega (\nabla W_i \cdot \mathbf{f} + W_i s) = 0, \qquad i = 1, \ldots, N \tag{6}.$$

In fact, with our three coupled equations (1) and three dependent variables ψ, ϕ_n, ϕ_p, we now have $3N$ coupled non-linear equations in the $3N$ unknowns ψ_i, ϕ_i^n, ϕ_i^p, $i = 1, \ldots, N$. These are solved by the finite element code by means of a generalized Newton's method.

ADVANTAGES OF FINITE ELEMENT

Because the finite element method is an integral method, with only first derivatives appearing, many complications associated with boundary value problems disappear. First of all, surface effects, whether at a boundary between regions of the device (e.g. the junction) or at the physical surface of the device (e.g. surface recombination) are effectively a special case of bulk effects where the integrand includes a Dirac delta function to localize the effect to the boundary. The delta function converts volume integrals into surface integrals. Thus, surface recombination and interface charge density may be handled easily by including surface integrals in equation (6). In addition, the perennial problem of matching the electric field at a jump discontinuity of ϵ does not even come up, having been integrated out of existence. Thirdly, multiple non-interacting recombination levels are dealt with simply by including additional terms in R (which appears in the s in equation (6)). Finally, non-rectilinear elements are readily handled by performing the integrations in (6) numerically.

IMPLEMENTATION

We have implemented a one-dimensional prototype of FIESTA ROC in C, running on an IBM-PC compatible and on a Cray XMP. The prototype features automatic mesh generation and automatic dark and light I–V simulations, as well as spectral response. Arbitrary numbers of recombination levels, degenerate statistics, and heavy doping effects are supported. Finite surface recombination velocities, as noted earlier, are imcompatible with our choice of boundary conditions in the one-dimensional case, so they have been left out of the prototype. Once the solution to equation (6) has been found for a given bias and illumination, many quantities of interest can be examined at any point in the cell. These include the electron and hole current densities, electric field, electric potential and quasi-Fermi potentials, net recombination, n, and p.

EXAMPLE

As an example of the use of FIESTA ROC, we have modeled an InP shallow homojunction n^+pp^+ cell from Spire Corporation which has been extensively studied with analytical models [2]. The growth parameters and modeling parameters found in [2] are reproduced in Tables I and II. Without any change in the parameters of either table, the results of light I–V and spectral response simulations by the prototype are shown in Figures 1 and 2. In addition, the measured and calculated solar cell parameters are shown in Table III.

Table I: Growth Parameters for Spire 6 Cell

emitter width	400 Å
n^+ emitter doping (Si)	1×10^{18} cm^{-3}
base width	3 μm
p base doping (Zn)	2×10^{16} cm^{-3}
BSF width	250 μm
p^+ BSF doping (Zn)	5×10^{18} cm^{-3}
cell area	0.25 cm^2
grid shadowing	4.8%

Table II: Modeling Parameters for Spire 6 Cell [2]

indirect lifetime of holes in emitter	2.0 ns
hole mobility in emitter	75 cm^2/V-s
indirect lifetime of electrons in base	150 ns
electron mobility in base	3988 cm^2/V-s
indirect lifetime of electrons in BSF	0.60 ns
electron mobility in BSF	2456 cm^2/V-s

The real utility of a numerical solver, however, lies in its ability to show what is happening in various regions of the cell. In this respect, it functions as a sort of computational microscope, allowing the investigator to probe all regions of the cell to determine, for example, which contribute most to the total recombination, light-generated current, and so on. In Figure 3, we show the calculated net recombination for three different bias points—short circuit, maximum power, and open circuit—plotted against the spatial coordinate x. Here $x = 0$ represents the metallurgical p-n junction and $x = 3\mu$m the base-BSF low-high junction. The emitter, being only .04μm wide, is invisible on this scale. The junction space charge region is visible as a low-recombination valley at short circuit and a high-recombination peak under forward bias. Note, however, the additional peak in recombination in the BSF region. In Figure 4, we show the same curve, at maximum power only, calculated for the same cell and for another differing only in the doping in the BSF, namely 5×10^{17} rather than 5×10^{18} cm^{-3}. The indirect recombination lifetime in the BSF is also correspondingly higher (6.0 ns instead of .60). The peak in the BSF almost disappears when the BSF doping is decreased. Such an analysis can aid cell fabricators in designing and producing more efficient cells.

CONCLUSIONS

We have demonstrated a one-dimensional prototype of a flexible finite element package that will enable cell designers to simulate a variety of effects and to pinpoint problems in proposed or existing cells. The two- and three-dimensional versions are currently under development.

REFERENCES

[1] Markowich, Peter. *The Stationary Semiconductor Device Equations*, Springer-Verlag, Vienna, 1986.

[2] Thesling, William. "Theoretical Modeling, Optimal Design and Performance Predictions of the Shallow Homojunction Indium Phosphide Solar Cell in Space Applications", Master's Thesis, Cleveland State University, Cleveland, Ohio, August 1990.

Table III: Solar Cell Parameters for Spire 6 Cell

	Measured	Calculated
I_{sc}, mA	8.47	8.37
V_{oc}, mV	868	869
I_{max}, mA	8.19	8.03
V_{max}, mV	751	754
FF, %	83.8	83.3
η, %	17.94	17.64

at 1AM0, 25°C

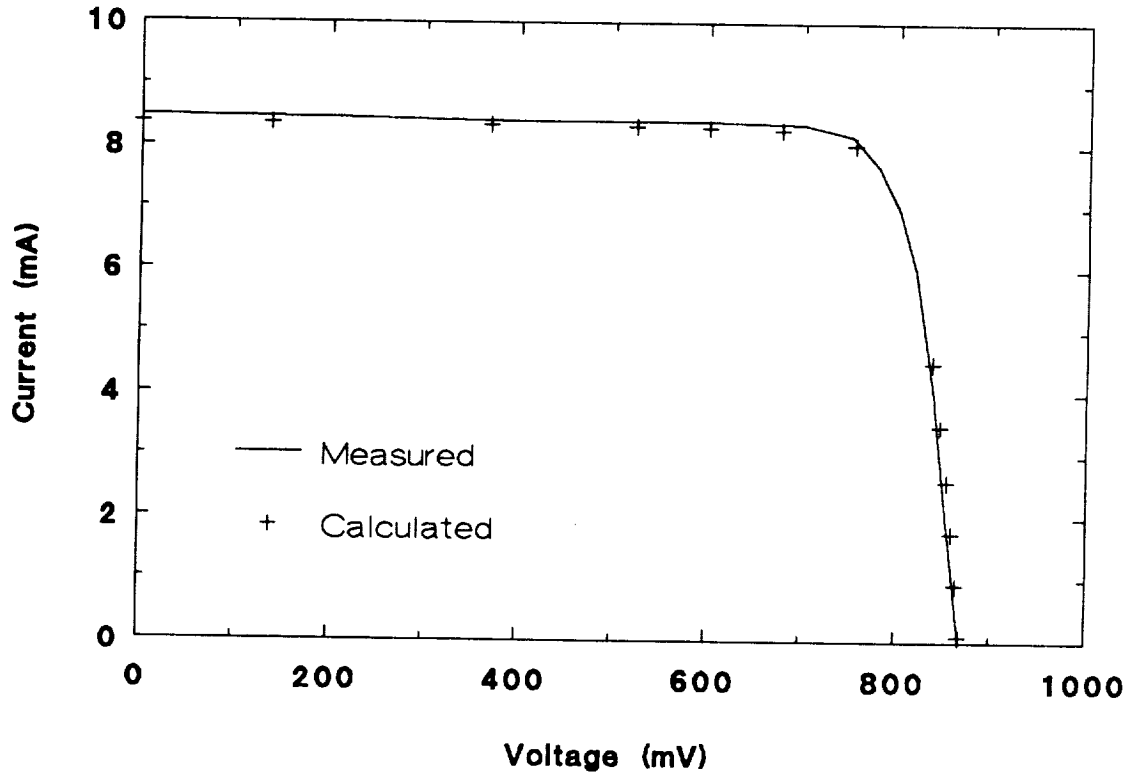

Figure 1: Illuminated I-V characteristic for cell Spire 6, with calculated results by FIESTA ROC prototype.

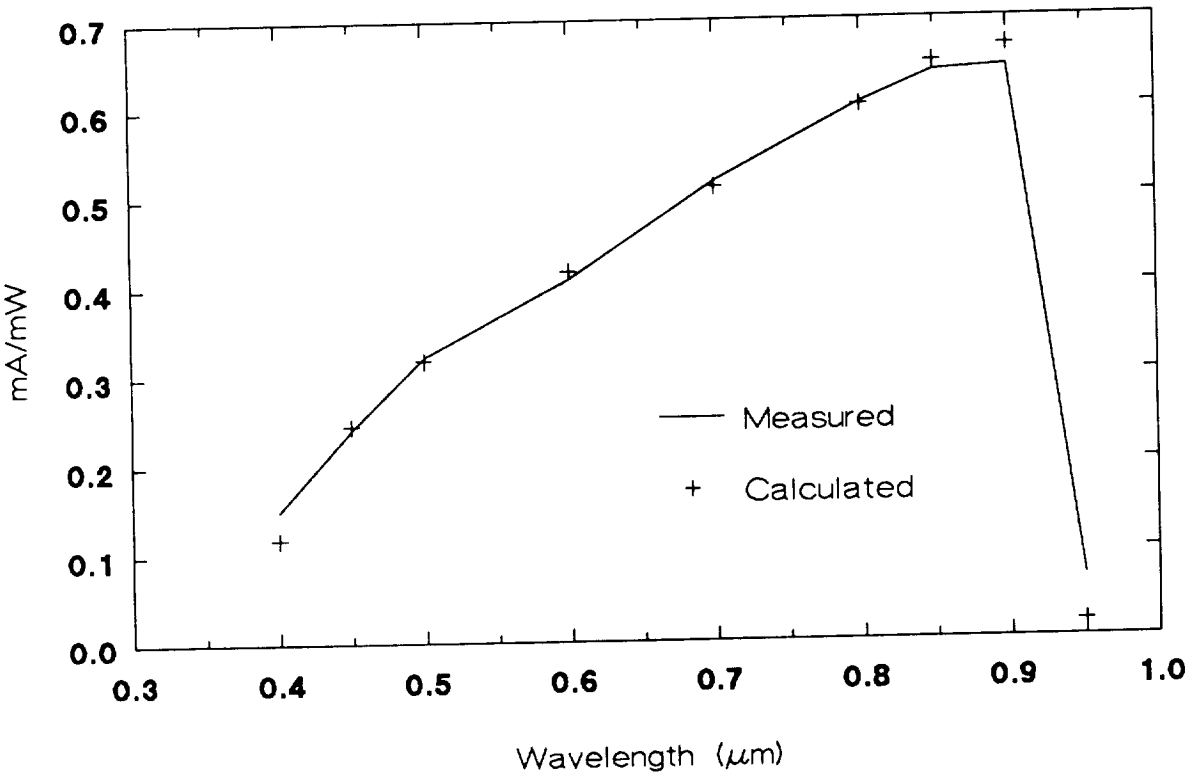

Figure 2: Spectral response for cell Spire 6, with calculated results by FIESTA ROC prototype.

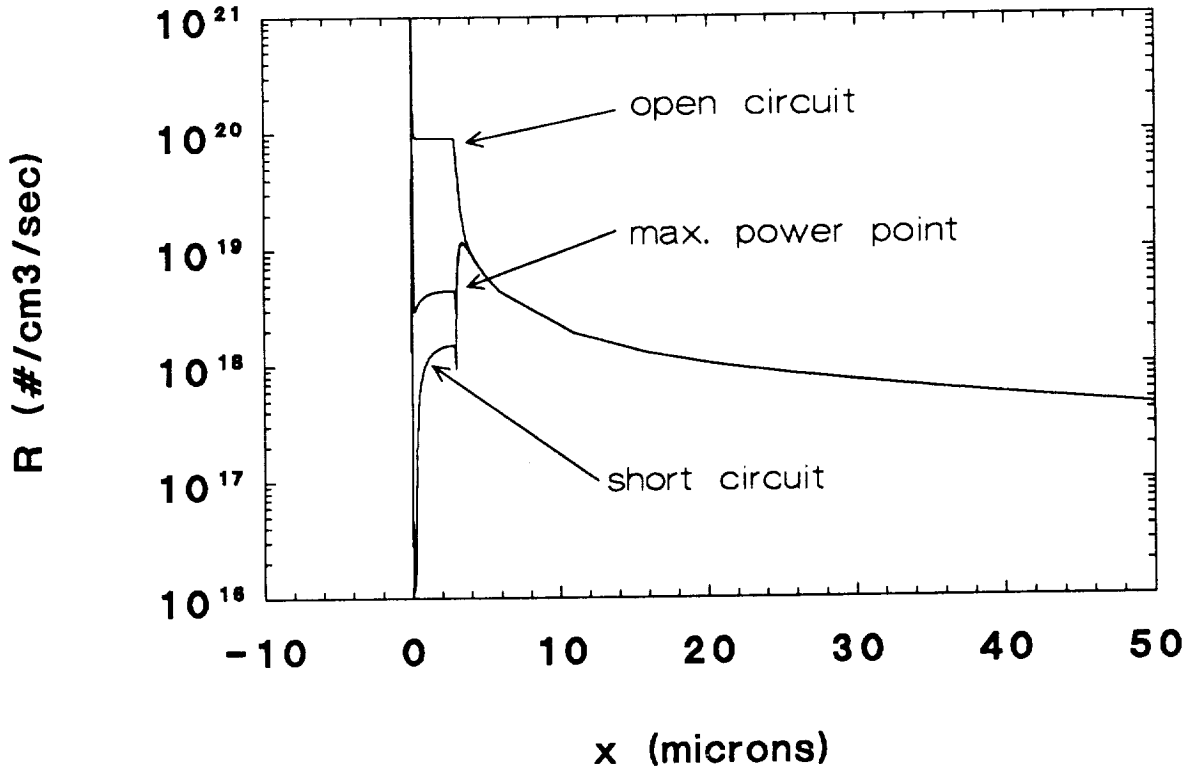

Figure 3: Net recombination calculated by FIESTA ROC prototype at three bias conditions. The n^+p junction is at $x = 0$ and the pp^+ junction at $x = 3\mu$m.

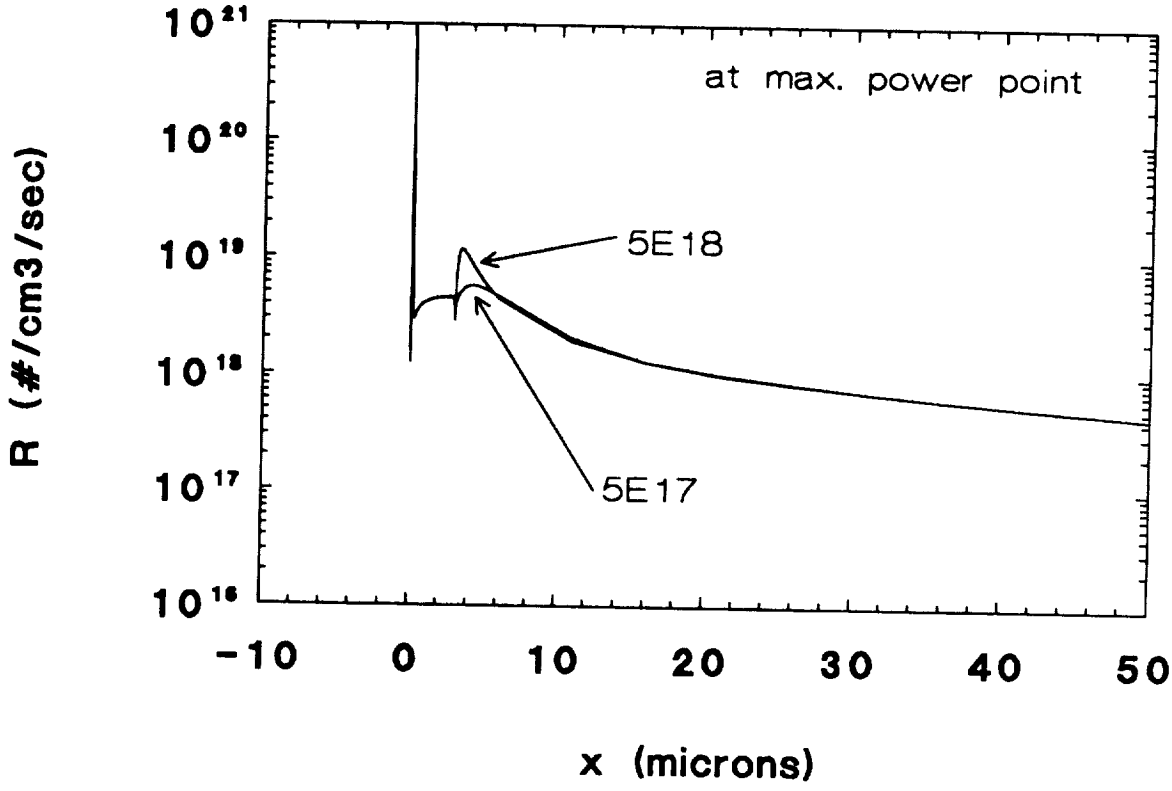

Figure 4: Net recombination calculated at max power voltage for cells with different BSF dopings.